Kuwait J.Sci., Vol.49, No.(2),April.2022,pp(1-11)

Thermodynamic Assessment of High Entropy (Fe-Mn) Binary Alloy System Using Calphad Method

Waseem Ullah Shah[1], Dil Faraz Khan[1], Haiqing Yin[2], Athanasios G, Mamalis[3]

[1]Dept. of Physics, University of Science and Technology Bannu, 28100, KPK, Pakistan
[2] School of material science and engineering, University of Science and Technology Beijing 100083, Beijing P.R China
[3] Project center for Nanotechnology and advance Engineering (PC-NAE), NCSR\Demokritus', Athens, Greece
Corresponding Author: waseemullahshah303@gmail.com

Abstract

The thermodynamic analysis and calculations of the high entropy metastable binary alloy iron-manganese system have been carried out using the CALPHAD (Calculation of Phase Diagram) method THERMO-CALC (thermodynamic calculations) package and FEDATE database. The thermodynamic analysis contains the assessment and estimate of the phase diagram, Gibbs energy of mixing, excess Gibbs energies, thermodynamic molar activities, coefficient of activities, partial and integral values of Enthalpy for Fe-Mn alloy system at three elevated temperatures 1200K, 1225K, and 1250K. The entropy of the said alloy system is calculated by showing linear accordance with temperature. The sudden increase is found in the enthalpy curve due to the overlapping of grain boundaries of the system. The Enthalpy offers to increase the alloy system's heat contents with a rising temperature range. The alloy shows a positive deviation from Vegard's law, Henry's law, and the corresponding negative deviation from Raoult's ideal Gibbs curve. The obtained results show that the ferromagnetic states of Fe-Mn alloy are the most stable state FCC_A1#1. For Mn and Fe system, the phase equilibria show activity curve data for the solid-state and show ideal characteristics behaviors. A small positive deviation from Henry's law was observed from the perfect curve. The alloy offers equilibrium and good stability.

Keywords: CALPHAD method; FEDAMO database; phase diagram; Thermodynamic calculations.

1. Introduction

For the significant evolution of twinning induced porosity (TWIP) based steels, the manganese is recognized as a well-applied element with great strength and flexibility [1]. Studied the lattice stability of manganese and iron was as alloying through the calculation of the phase diagram (Calphad) method. For four decades, the Calphad process has simulated, modeled, and developed thermodynamic properties of many metallurgy-based materials [2-3]. Researchers studied and

predicted the Calphad based profile of the ferric-manganese binary alloy system [4]. Tiller and Rao first described the thermodynamic-based chemical analysis of the Fe-Mn alloy system. The current research is carried for the Fe-Mn system by using the third generation Thermo-Calc software with special modules and databases and the Calphad method. The enthalpy transformation rules assessed the Fe-Mn binary system, and the Calphad optimization is carried out for gamma phase transformation. The transformation-wise phase like martensitic is studied for ferric-based alloys regarding the sigma phase, ferrite phase, and Gibbs energy [5-7]. The binary phase operation of the eutectoid is seen as less significant for phase transformation [8]. The sigma phase contributes to the Fe-Mn alloy system's magnetic sites properties at lower eutectoid temperature operations. The activity of Fe-Mn alloy shows some positive deviation and corresponding negative deviation. The Calphad assessment tool is highly used to calculate and model alloying systems [9]. The present research data and results agree with available experimental results and previous assessments by [10] Hue *et al*.

2. Phase diagram and method

The phase-based transformation in the Ferric-manganese system shows the FCC-A1 phase with ferrite-based configuration. BCC-A2 as an austenite-based phase. FCC-A1/HCP-A3 indicates the martensitic phase following the phase diagram calculated by Hue in 1987. The Ferric-Manganese system with all solution phases as liquid, BCC-A12, BCC-A2, CUB-A13, FCC-A1, CPH-A3, CPH-A3 phase shows high entropy-based metastable nature, and all the steps have calculated by Redlich-Kister polynomial calculations as following Hue and Lee in 1987 and 1989 respectively [11]. The manganese is a transition. Base metal is highly used in the magnetic base industries. The CPH-A3 phase being metastable creates homogenous heterogeneity in the phase structure of the system and makes variational-based characteristics for the solid solution. The research analysis shows that the ferromagnetic state of the ferric manganese is the most stable phase that exists in the ground state [12]. For Manganese and Ferric system, the phase equilibria show activity curve data for solid in almost ideal behavior with small positive deviation from ideality [13]. Following Hallowell's recommendations, a stable phase diagram for the Fe-Mn system has been investigated. Due to transition-based elements of the said alloy system, their magnetic properties are very complex and highly based on alteration of thermal energy and Curie temperature. The complex nature magnetism creates stable properties in that alloy system with low-temperature ranges.

$$G^{q} = x_{Fe}{}^{0}G_{Fe}{}^{q} + x_{Mn}{}^{0}G_{Mn}{}^{q} + G_{m}{}^{q} + G_{mag}{}^{q} \quad \textbf{(1)}$$

Where G is the Gibbs free energy of a system is for pure element, for Mn, Fe, Gibb's energy paramagnetic state value is 298.15K., while the other parameters x, Gm^{q} molar fraction, molar Gibbs energy, and magnetic-based ordering of the system,

$$G_{m}{}^{q} = RT\,[x\mathrm{Fe}\ln x\mathrm{Fe} + x\mathrm{Mn}\ln x\mathrm{Mn}] + G^{qs} \quad \textbf{(2)}$$

R is gas constant with excess molar Gibbs energy. Redlich-Kister power series is used for mathematical calculations as

$G_N^{q,\,s} = xFe\ xMn \sum^{n}_{v=0} L^{q}Fe, Mn\ (xFe - xMn)^{v}$ **(3)**

Now by Calphad convention rule

${}^{v}L^{q}Fe, Mn = a_v^{q} + b_v^{q}T + c_v^{q}T\ lnT + d_v^{q}T^{2} + e_v^{q}T^{3} + g_v^{q}T^{-1} + g_v^{q}T^{7} + h_v^{q}T^{-9}$ **(4)**

With "a" and "h" as imperial parameters.

Here the bcc-A2 of the ferromagnetic phase shows the magnetic contribution to this system, bcc-A12, cph-A3, fcc-A1, while cph-A3 shows anti-ferromagnetic contributions to this system, as by Hillert and jarl[14]**.**

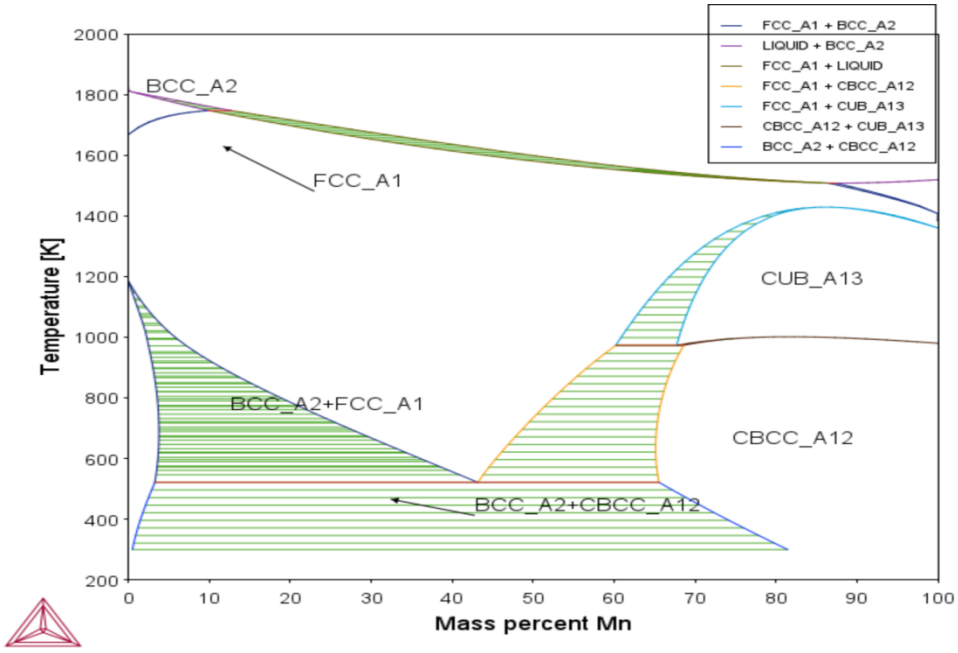

Fig. 1. Phase diagram of Fe-Mn binary alloy system at elevated temperatures.

$G_{mag}^{q} = RT \ln (B^{q} + 1)\ g\ (t)$ **(5)**

While for numerical solution, if g (t) <1 then we will observe as

$g\ (t) = 1-(79^{t-1}/140\ p + 474/497(1/p - 1)\ (t^{3}/6+t^{9}/135 + t^{15}/600))/D$ **(6)**

$G\ (t) = -\ (t^{-5}/10 + t^{-15}/315 + t^{-25}/1500)/D \quad$ if $\quad t > 1$ **(7)**

While $D = 0.46044 + 0.73189(1/\ (p - 1))$ **(8)**

$t = T/T^{q}_{C,N}$ that represents a particular curie temperature of q-Th phase during transformation from ferromagnetic to paramagnetic transformation, the value of P is 0.40 for bcc-A2,while for fcc-A1,BCC-A12,CPH-A3 are 0.38.so

$C_{pmag}^{q} = R \ln (Bq + 1)\ c\ (t)$ **(9)**

$C(t) = 474/497(1/p - 1)\,(2r^3 + 2t^9/3 + 2t^{15}/5))\,D$ if $t < 1$ **(10)**

$C(t) = (2t^{-5} + 2t^{-15}/3 + 2t^{-25}/5)/\,D$ if $t > 1$ [15-16] **(11)**

The proposed prediction in the Ferric-manganese alloy system shows the contribution to the ferromagnetic and anti-ferromagnetic phases and their transformation as the following literature through the Calphad method.

3. Thermodynamic modeling/simulations

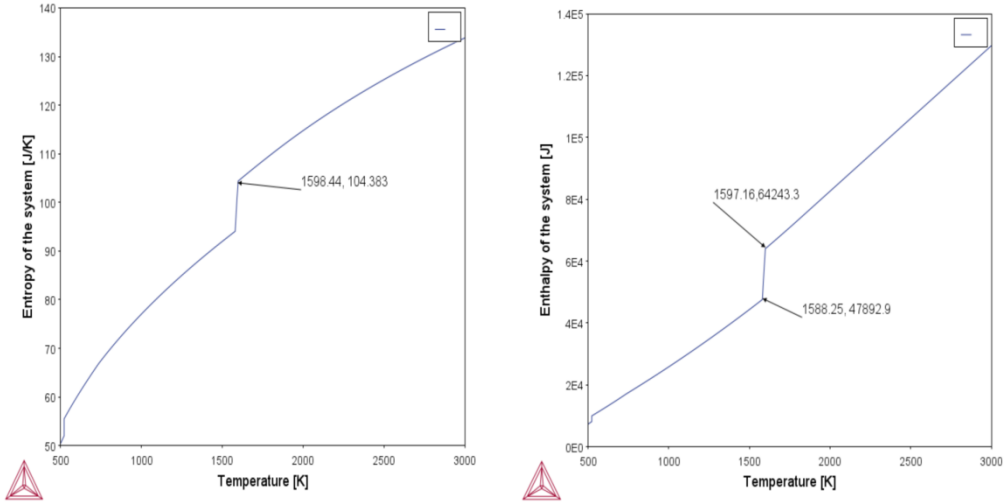

(a) (b)

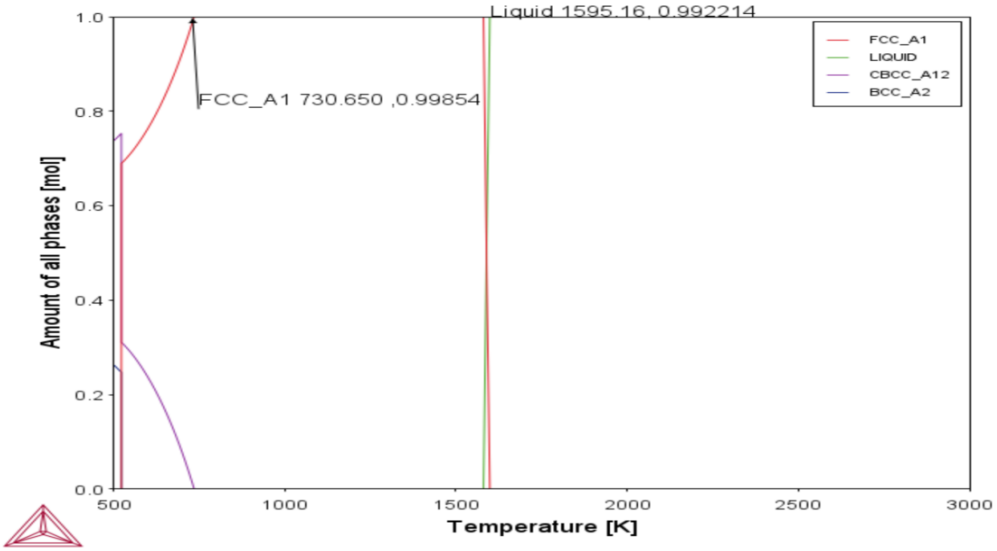

(c)

Fig. 2 (a, b, c). Shows Enthalpies, entropy, and phase profile of the Fe-Mn system at Elevated Temperatures.

Table 1. Shows entropy, Enthalpy of the binary Fe-Mn system at an elevated temperature range using FEDAMO.

Tempearture:^{0}K	Entropy: J/K	Tempearture:^{0}K	Entropy: J/K	Entropy: J/K
1350.00000	87.87676	1500.00000	91.96556	105.80675
1360.00000	88.15794	1510.00000	92.22900	106.07926
1370.00000	88.43781	1520.00000	92.49140	106.35079
1380.00000	88.71639	1530.00000	92.75317	106.62134
1390.00000	88.99371	1540.00000	93.01459	106.89095
1400.00000	89.26978	1550.00000	93.27557	107.15964
1410.00000	89.54462	1560.00000	93.53606	107.42743
1420.00000	89.81824	1570.00000	93.79599	107.69434
1430.00000	90.09067	1580.00000	94.05533	107.96039
1440.00000	90.36192	1580.28570	94.06273	108.22561
1450.00000	90.63201	1598.79477	94.06273	108.49001
1460.00000	90.90095	1598.79477	99.76004	108.75362
1470.00000	91.16876	**1598.79477**	**104.39497**	109.01646
1480.00000	91.43545	1600.00000	104.39497	104.42853
1490.00000	91.70105	1610.00000	104.39497	104.70633
1620.00000	**105.39497**	1660.00000	105.70634	107.70657
1630.00000	106.39797	1670.00000	106.70654	109.70685
1640.00000	107.39797	1680.00000	107.70654	110.70677
1650.00000	108.39797	1690.00000	107.70654	111.70678

Table 1 shows the entropy of the system versus the temperature profile. The entropy is found fluctuation based regularly with increasing the temperature profile. The response of entropy with temperature is nearly linear. The nonregularity is found at temperature ranges (1598K, 1620K) with values (104.39497J/K, 105.39497J/K). The composition curve shows that the system is highly entropy-based. The nonregularity in a given temperature and composition shows some rare doping behavior of the said alloying system. The method with the highest value in entropy at a given temperature shows the system's internal capability of doping resistance. The system responds to

the temperature regularly with a composition profile. The given temperature provides the system with the required coercing lattice energy that generates by weakening the grain boundaries at that profile temperature.

Table 2. The enthalpy calculations of the binary alloy system Fe-Mn system.

Temparature:^{0}K	Enthalpy:J/Mol	Temparature:^{0}K	Enthalpy: J/Mol
1350.00000	1.00007E5	1598.79477	1.07528E5
1340.00000	1.00477E5	1598.79477	1.07998E5
1330.00000	1.00947E5	1598.79477	1.08468E5
1320.00000	1.01417E5	1600.00000	1.08938E5
1310.00000	1.01887E5	1610.00000	1.09408E5
1300.00000	1.02357E5	1630.00000	1.09878E5
1520.00000	1.02827E5	1640.00000	1.10349E5
1530.00000	1.03297E5	1650.00000	1.10819E5
1540.00000	1.03767E5	1660.00000	1.11289E5
1550.00000	1.04238E5	1670.00000	1.11759E5
1560.00000	1.04708E5	1680.00000	1.12229E5
1570.00000	1.05178E5	1690.00000	1.12699E5
1580.00000	1.05648E5	1700.00000	1.13169E5
1580.28570	1.06118E5	1710.00000	1.13639E5

Table 2 shows the enthalpy calculations of the binary alloy system Fe-Mn system at a high-temperature range. The Enthalpy is increasing with increasing temperature. It shows that the heat contents of the system increase with increasing the repulsive interactions of the system of alloying elements. At 1588.25K, 1597.16K, with a composition profile of 47892.9, 64243.3 per mole, a specific change in Enthalpy is shown due to excessive collision and interactions of the Alloying elements. Due to repulsive interactions, the grain boundaries and lattice vibrations mode strongly interact with the temperature profile. Almost all the systems show the highest heat contents with increased temperature of the given binary alloy system Fe-Mn.

Table 3. Thermodynamic calculations of different phases in system Fe-Mn system at elevated temperatures

Temperature: degree Kelvin	Amount of BCC_A2 (Mole)	Amount of CBCC_A12 [mol]	Amount of FCC_A1 [mol]
1350.00000	1.00000	0.55116	1.000001710
1360.00000	0.44884	1.00000	1.000001720
1370.00000	0.00000	0.75298	1.000001730
1380.00000	0.24702	0.75116	1.000001740
1390.00000	0.24884	0.74409	1.000001750
1400.00000	0.25591	0.73711	1.000001760
1410.00000	0.26289	1.00000	1.000001770
1420.00000	1.00000	0.98807	1.000001780
1430.00000	0.01193	0.96517	1.000001790
1440.00000	0.03483	0.94337	1.000001800
1450.00000	0.05663	0.07738	1.000001810
1460.00000	0000 00	0.90287	1.000001820
1470.00000	0.09713	0.88407	1.000001830
1480.00000	0.11593	0.86617	1.000001840
1490.00000	0.13383	0.84914	1.000001850
1500.00000	0.15086	0.83294	1.000001860
1510.00000	0.16706	0.18246	1.000001870
1520.00000	0.19710	0.81754	1.000001880
1530.00000	0.21099	0.80290	1.000001890
1540.00000	0.22417	0.78901	1.000001900

Table 3 shows the thermodynamic calculations of different phases and composition ranges for the binary alloy system Fe-Mn binary system. Austenite standard CBCC_A12 phase is the most temperature surviving one in a solid era with the highest composition profile. The calculation shows that the austenite phase is the most stable in the phase profile diagram of the Fe-Mn system. There is a temperature-wise best response in all the phases, but the Austenite and the ferrite are best. The liquid phase is in couple with the ferrite phase with little composition profile.

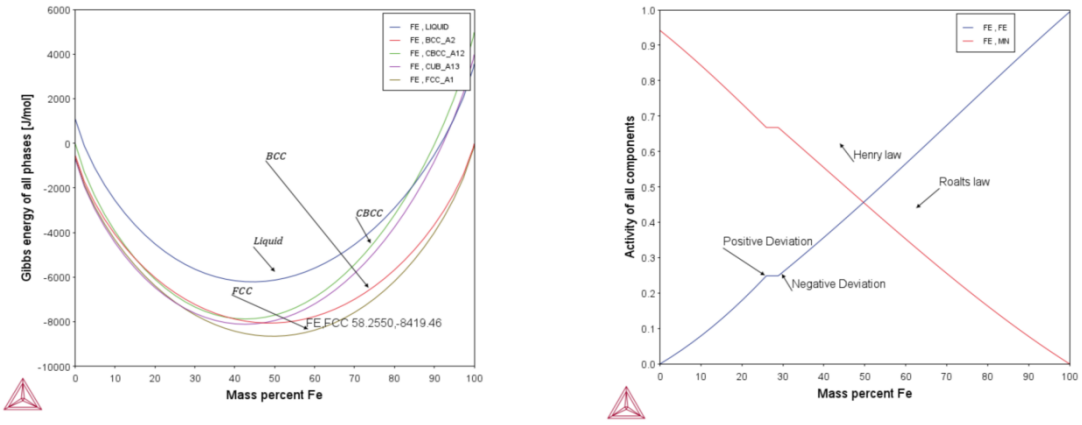

(a) (b)

Fig. 3 (a, b). shows Gibbs energy, Molar Activity of the Fe-Mn system at elevated temperatures.

Table 4. Database thermodynamic phase calculation at temperature: 1200K, 1225K, And 1250K for the system: **Fe-Mn**

T=K^{O}	Pressure: pascal	Number of moles	the activity of a relative component ratio (Mn)	Mass: gram	Total Gibbs energy: J/mol	Volume :cm3	Enthalpy:j/mol	Activity Fe. SER: stable element reference state	Activity Mn. SER: steady element reference state
1200 K	1.000000*10^5	1.00000*10^0	1000000*10^{-2}	5.58378*10^1	-5.72895*10^4	7.22772*10^{-6}	3.50202*10^4	9.8984*10^{-1}	1.0164*10^{-2}
--	--	--	--	--	--	--	--	9.9000*10^{-1}	1.0000*10^{-2}
--	--	--	--	--	--	--	--	3.3925*10^{-3}	1.4088*10^{-5}
--	--	--	--	--	--	--	--	-5.6733*10^4	-1.1145*10^5
FCC_A1#1	--	1.0000*10^0	--	5.5838*10^1	--	--	--	--	--
--	--	--	--	--	--	--	--	9.90000E-01	1.00000*10^{-2}
1225 K	1.000000*10^5	1.00000*10^0	1*10^{-2}	5.58378*10^1	-5.92215*10^4	7.24094*10^{-6}	3.58762*10^4	9.8984*10^{01}	1.0164*10^{-2}
--	--	--	--	--	--	--	--	9.9000*10^{-1}	1.0000*10^{-2}
--	--	--	--	--	--	--	--	3.1547E-03	1.3321E-05
--	--	--	--	--	--	--	--	-5.8656*10^4	-1.1434*10^5
FCC_A1#1	--	1.0000*10^0	--	5.5838*10^1	--	--	--	9.90000*10^{-1}	1.00000*10^{-2}
1250 K	1.000000*10^5	1.00000*10^0	--	5.58378*10^1	-6.11710*10^4	7.25418*10^{-6}	3.67375*10^4	9.8984*10^{-1}	1.0164*10^{-2}
--	--	--	--	--	--	--	--	9.9000*10^{-1}	1.0000*10^{-2}
--	--	--	--	--	--	--	--	2.9372*10^{-3}	1.2600*10^{-5}
--	--	--	--	--	--	--	--	-6.0595*10^4	-1.1725*10^5
FCC_A1#1	--	--	--	--	--	--	--	9.90000*10^{-1}	1.00000*10^{-2}

Table 4: Shows thermodynamic calculations and results of Ferric-Manganese during alloying. For 1200K, the Gibbs energy of the alloying gets a value of -5.72895*10^4 J/mol. The Enthalpy of the system gain value of 3.50202*10^4 J/mol corresponding to Gibbs energy.The molar activity of Ferric and Manganese is changing a values (9.8984*10^{-1},9.90000*10^{-1},3.3925*10^{-3},-5.6733*10^4 ,9.9000*10^{-1}), (1.0164*10^{-2} ,1.0000*10^{-2},1.4088*10^{-5} ,1.00000*10^{-2},-1.1145*10^4) while the

existing phase is FCC-A1#1 with high stability as ferrite one. For1225K, the Gibbs energy got a value of -5.92215*10^4 J/mol with a further decreasing value, while Enthalpy acquired a more positive value of 3.58762*10^4J/mol. The molar activity fluctuation is for Fe, Mn element as (9.8984*10^{-1},9.9000*10^{-1},9.90000*10^{-1},-5.8656*10^4,3.1547*10^{-3}),(1.0164*10^{-2},1.0000*10^{-2},1.00000*10^{-2},-1.1434*10^5,1.3321*10^{-5}) with FCC-A1#1 phase as a stable phase for the given temperature with ferrite coordination for 1250K of last temperature interval in our study the, Total Gibbs energy reaches its highest negative value of -6.11710*10^4J/mol and highest positive value of Enthalpy 3.67375*10^4 J/mol indicates that the system is going toward most stability even if the repulsive interaction is more active. Thermodynamic molar Activity of Fe, Mn elements are highest values as(9.8984*10^{-1},9.9000*10^{-1},2.9372*10^{-3},9.90000*10^{-1},-6.0595*10^4),(1.0164*10^{-2},1.0000*10^{-2},1.00000*10^{-2},-1.1725*10^5 ,1.2600*10^{-5}) with highest stable phase in the phase diagram FCC-A1#1 as ferrite coordination . The activity of Ferric is maximum as (9.90000*10^{-1}) while smaller for Manganese elements. The Fe-Mn system is more reliable instability and industrial needs at the highest temperature with nonequilibrium properties.

4. Conclusion

The thermodynamic assessment is given for the ferric-manganese system through the Calphad method with pbine, FEDAMO databases. The thermo-calc software is used for all simulations and modeling. The calculation seems to optimize fluctuation and phase transition due to magnetic properties and compositional heterogeneity. The alloy shows high entropy-based metastable properties with having no equilibrium following the literature. The Enthalpy increases linearly with increasing the alloying temperature, resulting in a gradual increase in repulsion forces among elements. The alloy shows positive deviation from Vegard's law following the literature. The Gibbs energy of the alloy decreases gradually, which results in the stability of the said alloying system and reports negative deviations from Raoult's law ideal curve. According to Raoult's law, the total Gibbs energy decrease with temperature shows more system stability. The highest negative deviation from Raoult's law is seen at 1250 K in the Ferric-Manganese system, increasing the alloy's stability level. Calculations results enhance the hardness, wear resistance, corrosion resistance, and other alloy's doping characteristics. The ferromagnetic phase is the stable phase and occupies at ground level in the said alloy system as the following literature. The measured phase transformation equilibria activity curves show exemplary behavior with a small positive deviation from henrys law. Following Hallowell's recommendations, a stable phase diagram for the Fe-Mn system has been investigated. The complex magnetic properties of the alloy are due to the transition behavior for the metals and can be enhanced by the alteration of coercive thermal energy and temperature. The entropy and enthalpy proportion of the alloy at 1250K is responsible for the high heat-absorbing capacity of the Fe-Mn alloys system. The throughout fluctuation inactivity is by Vegard's and Henry’s law and results in rare doping characteristics for the greater industrial need and research areas.

References

A.T. Dinsdale. (1991). "Scientific Group Thermo-data Europe Database for Pure Elements," Calphad journal. (15):317-425.

B. Lee, D.N. Lee. (1993). a thermodynamic evaluation of the Cr-Mn and Fe-Cr-Mn systems, (24)**:**919-1933.

E.J. Mittemeijer. **(2004).** Reevaluation of the Fe-Mn Phase Diagram, Journal of Physics EDAV, (25)**:**346-354.

G.M. Stocks, W.A.Shelton. (2002). on the magnetic structure of Y-Fe-Mn alloys. Journal of Applied. Physics. (91**)**: 7355-3490.

I. Ansara, M.H. Rand. (1998). COST-507. Thermochemical Database for Light Metal Alloys Scientific Group Thermo-data Europe Database, EUR (2):18499.

J. Martinez, S.M. Cotes, J. Desimoni. (2009). Enthalpy change of the HCP/FCC martensitic Transformation in the Fe–Mn and, Journal of Alloys and Compound. (479):204–209.

J. Nakano, P.J. Jacques. (2010). It affects the thermodynamic parameters of the hcp phase on the stacking fault. Journal of Calphad (34**)**:167–175.

J.Vrestzal, Jana Pavlu. (2002). Energetic and phase diagrams of Fe-Cr and Co-Cr systems from first principles, (38**)**:3-4.

Lacaze. Jacques and Elena. (2010). Thermodynamic assessment of the aluminum corner of the Al-Fe-Mn-Si, mat and mater Trans, (41)**:**2208-2215.

Lina Kjelqvist. (2008). Thermodynamic descriptions of the Fe-C-Cr-Mn-Ni-O system Calphad, (32)**:**577-592.

Lina Kjelqvist. (2009). Thermodynamic description of the Fe-C-Cr-Mn-Ni-O system, materialvetenskap KTH, Stockholm, ISBN 978-19-7415-428-3.

M. Selleby. (2015) Thermodynamic database for Highmanganese steels simulations, Calphad journal, Italy.

Satoshi Matsumoto, Tatsuya Tokunaga. (2005). Thermodynamic analysis of the phase equilibria of the Nb-Ni-Ti system, (46)**:**2920-2930.

T. Gebhardt, D. Music, B. Hallstedt, M. Ekholm, I.A. Abrikosov, L. Vitos, J.M. Schneider. (2010). Ab initio lattice stability of FCC and hcp Fe–Mn random alloys, Journal of Phys: Condens. Matter, (22)**:**295-402.

Tatsuya Tonnage *et al*, (2008). Thermodynamic analysis of the phase equilibria in the Fe-Zr-B system, Calphad journal, (11):2534-2540.

V.T. Witusiewicz, F. Sommer, E.J. Mittemeijer. (2004). Reevaluation of the Fe-Mn phase diagram, Journal of. Phase Equilib Diffus. (25**):**346–354.

Submitted: 05/02/2020
Revised: 09/04/2021
Accepted: 23/04/2021
DOI: 10.48129/kjs.11303